

Corrosion behavior of nanohybrid titania–silica composite coating on phosphated steel sheet

A. K. Guin, S. K. Nayak, T. K. Rout,
N. Bandyopadhyay, D. K. Sengupta

© ACA and OCCA 2011

Abstract Corrosion resistance behavior of sol–gel-derived organic–inorganic nanotitania–silica composite coatings was studied. Hybrid sol was prepared from Ti-isopropoxide and *N*-phenyl-3-aminopropyl triethoxy silane. The structure, morphology, and properties of the coating were characterized by Fourier transform infrared spectroscopy (FTIR), scanning electron microscopy (SEM), and thermo gravimetric analysis. The corrosion performances of the sol–gel-coated samples were investigated by electrochemical impedance spectroscopy (EIS) and standard salt spray tests. The hybrid coatings were found to be dense, more uniform, and defect free. In addition, the coatings also proved its excellent corrosion protection on phosphated steel sheet.

Keywords Titania, Sol–gel, Coating, Corrosion, EIS

Introduction

Different types of steels are widely used in construction, automotive, and many other applications. However, steel when exposed to the environment gets corroded. Application of coating is the most generic way to protect metals from corrosion. Conventionally, chromate conversion coatings are being used to improve corrosion resistance as well as paint adhesion on metal substrates. However, due to environmental and carcinogenic problems associated with hexavalent chromium, the use of chromium is reduced and almost stopped. A number of alternate technologies have

been developed for corrosion prevention of steel substrates, which includes physical vapor deposition (PVD), chemical vapor deposition (CVD), electrochemical deposition, plasma spraying, painting, and sol–gel coatings. Among them, sol–gel coatings are gaining more importance as barrier coatings which prevent diffusion of the corrosive agents such as water, oxygen, and chloride ions to the coating/metal interface.^{1–3}

Nanostructure sol–gel coatings have shown a promising performance and can be used as an alternative to the chromate-based surface pretreatment.^{1,4–6} Among them, organic–inorganic hybrid coatings are of special interest due to their combined properties of organic polymers and inorganic ceramics.^{1,7–10}

The hybrid sol–gel materials provide the advantages of organic polymers (easy processing with conventional techniques, elasticity, and organic functionalities) with the properties of inorganic oxides (hardness, thermal and chemical stability, transparency).¹¹ Most of the organic–inorganic hybrid materials reported in literature are thermally cured^{12,13}; alternatively hybrid network materials can be prepared by radiation curing a UV-curable binder system.^{14,15}

The organic components allow tailoring of hydrophobicity, flexibility, functional compatibility and toughness, whereas the inorganic components improve the scratch resistance, density, abrasion resistance, high-thermal resistance, durability, and adhesion to the metal substrate due to the formation of covalent Me–O–Metal bonds. Moreover, incorporated inorganic nanoparticles can play the role of nanoreservoirs for storage and controllable release of the inhibitor species.^{5,16,17}

Inorganic–organic sol–gel coatings provide better adhesion than pure organic coatings, as the inorganic component of the precursors can easily react with metal substrates by the surface hydroxylation. As the name implies, there are two distinct stages during the

A. K. Guin (✉), S. K. Nayak, T. K. Rout,
N. Bandyopadhyay, D. K. Sengupta
Research and Development, Tata Steel Ltd,
Jamshedpur 831001, India
e-mail: akshya.guin@tatasteel.com

synthesis. This technique is based on the hydrolysis and condensation. In this process, the particles react with each other in such a way that the polymeric chains are formed and these chains develop three-dimensional structures. With further drying and heat treatment, the gel is converted into the dense ceramic particles.

Hybrid sol–gel materials can be prepared by incorporating nanoparticle or filler into the polymer matrix. Different physical, mechanical, and electrical properties can be modified by controlling the composition, size, and concentration of inorganic particles. Many studies have been reported on the use of different inorganic nanoparticles in the coating formulation for developing corrosion resistant coatings.¹⁸ Titanium is a well-known self-protective metal, as the impervious titania layer offers protection against many corrosive environments. Amorphous layer of titania coating inhibits oxygen reduction and does not allow the cathodic reaction of electrochemical corrosion process to start, thereby increasing the corrosion protection. Stability as well as performance properties, specifically barrier properties of titania nanocoating, can be enhanced by incorporating different silane groups. It has been extensively demonstrated that organosilane offers effective corrosion protection on steel substrate.^{3,18,19}

This article describes the formulation of nanotitanium coating by using *N*-phenyl-3-aminopropyl triethoxy silane as a coupling agent and an adhesion promoter. Role and performance of *N*-phenyl-3-aminopropyl triethoxy silane have been examined by Fourier transform infrared spectroscopy (FTIR) and scanning electron microscope (SEM) has been used to understand the surface morphology of coatings. Different performance of the coatings like flexibility, thermal behavior, and corrosion resistance properties, etc. are also evaluated and analyzed in this article.

Experiment

Preparation of sol–gel solution

The cold rolled and annealed (CRCA) steel sheets were used in the present study. These sheets were degreased to remove oil and grease (2% Ridoline 1352 BA, of M/s Henkel Chembond India Ltd.) and subjected to phosphating in tri-cationic phosphate base solution²⁰ to obtain a thin coating of <0.5 μm thickness (2–3 g/m^2).

The titania precursor was prepared by mixing titanium-isopropoxide and 2-methoxy glycol and acetyl acetone (AcAc) as outlined by Rout et al. and others.^{21–24} After 24 h of aging, *N*-phenyl-3-aminopropyl triethoxy silane was added slowly into the titania precursor in 1:1 (v/v) mixing ratio at room temperature (RT). Above synthesized sol–gel solution (mixture of titania precursor and *N*-phenyl-3-aminopropyl triethoxy silane) was applied on the phosphated sheet by the

dipping process and the dipping time was 1 min at RT, followed by slow drying at the rate of 20°C/m and finally dried at 150°C for 1 h.

IR spectroscopy study

Spectra of sol–gel solution was recorded on Fourier transform infrared spectrophotometer (Nicolet 5700, Thermo Electron Corporation) in the spectra range of 400–4000 cm^{-1} with a resolution of 4 cm^{-1} .

Particle size study

Particle size of 30 days aged sol–gel solution was measured in Nano ZS, Malvern Inst, UK by dynamic light scattering (DLS) method.

Contact angle measurement

An advanced sessile drop method was used for the contact angle measurement. The static contact angle of coated sample was determined by contact angle system (OCAH230 Dataphysics Instrument, Germany). Demineralized (DM) water was used as testing liquid.

Differential scanning calorimetry (DSC) study

Glass transition temperature (T_g) was calculated through DSC instrument (TA Instrument, Q10). Approximately 10 mg of 7 days cured film was taken in hermetic type pan and DSC runs were made at a heating rate of 10°C/m between 10 and 500°C under 50 mL/m nitrogen in a dynamic mode of operation. The T_g was determined from the second heating cycle.

Thermogravimetric analysis (TGA) and differential thermal analysis (DTA)

Approximately 10 mg of 7 days cured powdered sample was used for a thermal analysis study by a simultaneous TG-DTA analyzer (Shimadzu, DTG-60, Japan) in nitrogen environment. Heating rate was maintained at 10°C/m in the temperature range of 30–500°C.

Surface morphology analysis

The microstructural characteristics and coating thickness of sol–gel-coated steel samples were evaluated under a SEM (SUPRA 25, ZEISS FEG) equipped with energy-dispersive spectrometer (EDX) at an accelerated voltage of 15 kV and 2.8 A probe current with a working distance of 10 mm. The sample cross section was prepared as per Jordan et al.²⁵

Cupping test

The objective of this test is to identify the resistance of the coated film against ongoing deformation of a coated steel panel. The cupping test was done as per the ASTM E643-84. Initial disturbance (crack, mm) of the coating is recoded as cupping value.

Potentiodynamic polarization and electrochemical impedance spectroscopy study

Corrosion resistance properties of steel surface with and without sol–gel coating were investigated by potentiodynamic polarization and electrochemical impedance spectroscopy (EIS) test. EIS study was carried out in the frequency range of 100 kHz to 0.01 Hz. A typical three-electrode system was used in these tests: the samples act as the working electrode (1 cm² of exposed area), saturated calomel electrode (SCE) as reference, and graphite was used as a counter electrode. 3.5% aqueous NaCl solution was used as an electrolyte in all the measurements.

Salt spray test

Salt spray tests were carried out as per the ASTM B-117 test method. An unscribed sample of 3" x 3" size with 5–6 μm dry film thickness was exposed in a salt spray chamber. The panels were checked at regular interval of time and results were noted down in terms of blisters, creep, and red rust.

Results and discussion

FTIR study

The proposed reaction between titania precursor and coupling agent *N*-phenyl-3-aminopropyl triethoxy silane is shown in Fig. 1(a).

The IR spectra measured for the titania sol, *N*-phenyl-3-aminopropyl triethoxy silane, and sol–gel solution (mixture of titania sol and with *N*-phenyl-3-aminopropyl triethoxy silane) are shown in Fig. 1(b).

A shift in the wave number of the peaks and the presence of new peaks are indications of the breakage of existing bond and formation of new bonds. Free O–H stretching frequency in titania sol at 3403.2 cm⁻¹ has decreased after mixing/reacting with coupling agent (*N*-phenyl-3-aminopropyl triethoxy silane); which indicates the reaction of titania sol and coupling agent. The presence of Si–O–Si peak at 1000–1200 cm⁻¹ indicates hydrolysis of triethoxy group forming silanol group (Si–OH); subsequent condensation gives rise to a very stable Si–O–Si bond. The broad bands corresponding to Ti–O–Ti at 600–750 cm⁻¹ and Ti–O–Si at

930 cm⁻¹ reflect the good homogeneity of the hybrid coating.^{23,26,27} The presence of Ti–O–Si peak at 930 cm⁻¹ indicates the reaction has occurred between the free –OH of titania sol and that of free –OCH₃ group of the coupling agent.²⁴ There is no indication of Ti–O–N linkage in the given FTIR spectra, which indicates the delocalization of the nitrogen electron pair to the phenyl ring so that it is not available for donating to the vacant *d*-orbital of Ti. Another possibility is that phenyl groups (bulky in nature) present in *N*-phenyl-3-aminopropyl triethoxy silane hinder the donation of nitrogen lone pair to the vacant 3*d*-orbital of Ti. Si–O–Si, Ti–O–Ti, and Ti–O–Si peaks supported the proposed reaction between titania precursor and coupling agent (*N*-phenyl-3-aminopropyl triethoxy silane) as shown in Fig. 1(b). From the FTIR absorption peaks and the given reaction scheme, it has been observed that titania sol and coupling agents are creating a compact three-dimensional network of Ti–O–Ti, Ti–O–Si, and Si–O–Si by polycondensation of Ti(OH)₄ and the coupling agent resulting in adherence to the substrate through H-bonds and van der Waals bonds between functionalized titania particles and metal substrate immediately after application. The bonds can be transferred into stable covalent bonds during the densification/sintering process as shown in Fig. 2.^{28,29}

Particle size study

The stability of sol–gel solution is controlled by the rate of hydrolysis of titania sol. A fast reaction converts the reaction mixture into a gel-like mass and the sol–gel solution cannot be used for a longer period of time. Figure 3 shows the particle size distribution of 30 days aged sol–gel solution. It is found that particle size is in the range of 2–5 nm. This close size range is due to the controlled growth of hydrolysis and the condensation reaction of titania precursor. The addition of AcAc might have inhibited both hydrolysis and condensation reaction of titanium precursor thereby controlling the growth of the particles.³⁰

Contact angle study

The evaluation of the wetting properties, estimation of free surface energy, hydrophobicity of the noncoated and coated samples are assessed by contact angle measurement. Contact angle of the coated sample was found to be in between 78.8 and 81.8° (22.5–23.2° for uncoated sample) and corresponding surface energy measured by EOS method was found to be 38.13 × 10⁻⁹ N/m and coated surface is not wetted by water, i.e., coating imparts hydrophobicity to the metal surface. As the water molecules are not retained on the surface, due to hydrophobicity, corrosion is inhibited at the coated metal surfaces.

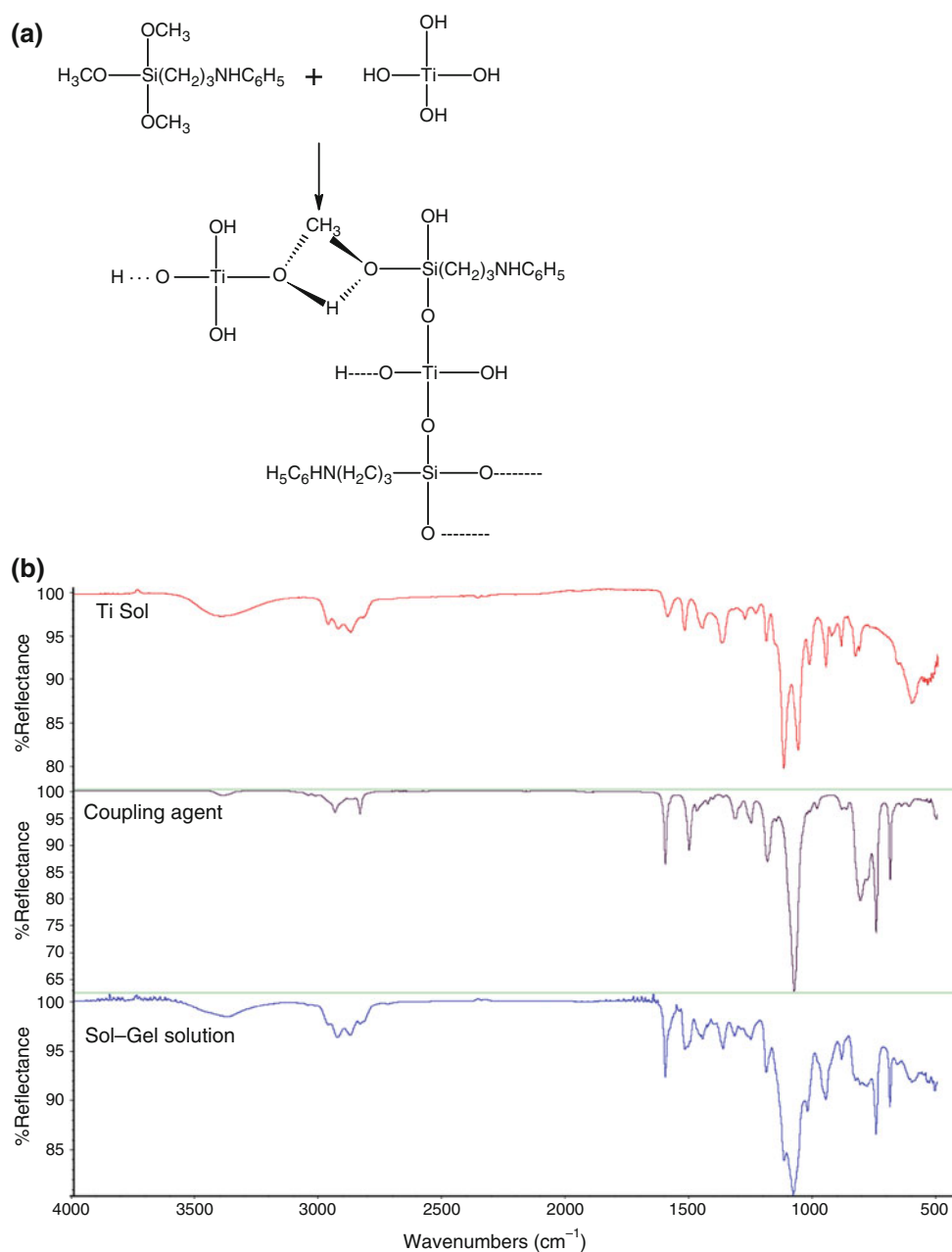


Fig. 1: (a) Probable reaction mechanism of Ti sol and coupling agent, and (b) FTIR spectra of sol, coupling agent, and sol-gel solution

Thermogravimetric study

The thermal stability of sol-gel coating has been measured by TG-DTA in nitrogen atmosphere with a heating rate of 10°C/min as shown in Fig. 4(a). The 5% loss of weight near 175°C can be attributed to the desorption of water and a part of the organics associated with the powder sample. A significant mass loss of (26.51%) and two isotherms have been observed at 410–420°C and 490–500°C, which may be due to desorption

and evaporation of organic components.¹ After 500°C, there is an abrupt weight loss, which is due to pyrolysis of the organic group. The T_g was found to be around 72°C. This high T_g of cured sample proves high rigidity and integral crosslinking network formed by titania and silane group. This integral crosslinking network creates a hydrophobic environment (contact angle 78–80°) for moisture, since these anions cannot penetrate easily through the coating and subsequently enhance the corrosion resistance of the coated metal surface.

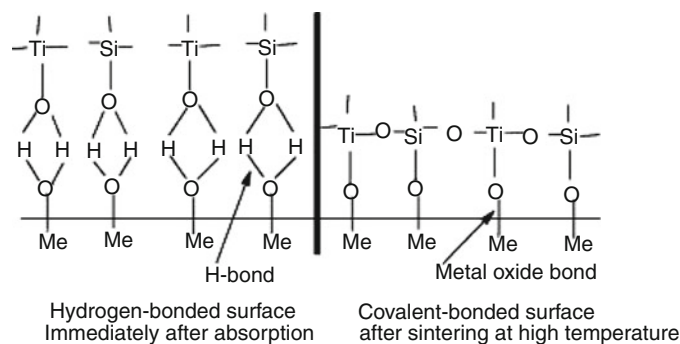


Fig. 2: Bonding mechanism before and after sintering of coating

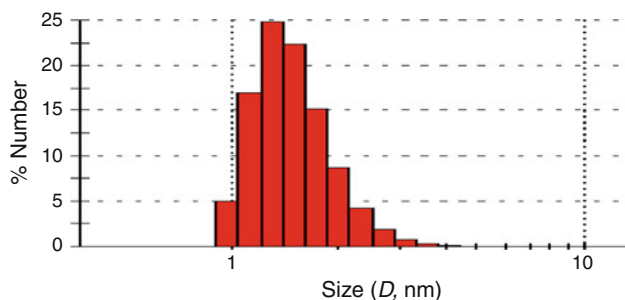


Fig. 3: Particle size distribution curve

Surface morphology study

Morphological characterization of coatings were done by SEM, and the surface morphology are shown in Fig. 5(a)–5(d). The figures indicate the presence of uniform, homogeneous, and crack-free hybrid sol-gel coating. Further titania and silicon are uniformly distributed and there is no agglomeration of nanotitania and silica particles in the polymer matrix. Cross-sectional view of the coated sample also shows the uniform coating layer and the coating thickness is found to be around 5–6 μm , Fig. 5(e) (eddy current method also supports the 5–6 μm coating thickness) EDX analysis of the coated sample as shown in Fig. 5(a), revealed that Ti and Si and/or their oxide completely covers the metal surface and there is no trace of iron peak detected. These types of compact arrangements of particles resist nucleation and extension of microcracks, resulting in better surface coverage, strength, and toughness.

Cupping test

The flexibility of the coating was evaluated by the cupping test; the results of which showed the high flexibility of the titania-hybrid sol gel coating. Titania sol-gel-coated surface and metal surface remain integrated at 7.6 mm cupping value. However, at 9 mm when metal cracks, sol-gel coatings remain adhered to the metal surface. This result indicates the strong cohesive and adhesive interaction between coating and metal surface. This high-flexibility property does not allow the coating to cracks prior to metal cracks. The SEM images also reveals that there is not much difference in the coated metal surface, even after 9 mm cupping value (Figs. 6a, 6b).

Corrosion resistance study

Before 200 h of salt spray test in ASTM B 117 chamber, there is no visible blister or coating defect observed on the coated surface (except a few localized

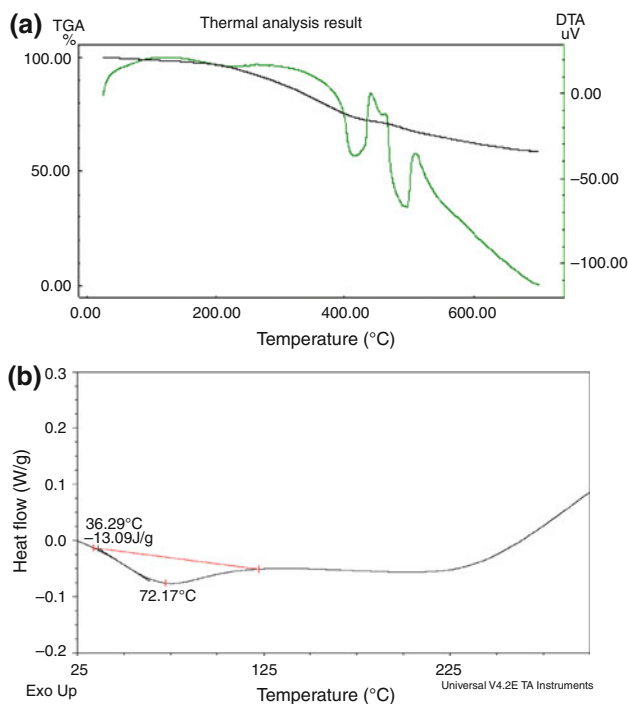


Fig. 4: (a) TGA analysis of Ti-hybrid-coated sample and (b) glass transition temperature of Ti-hybrid-coated sample

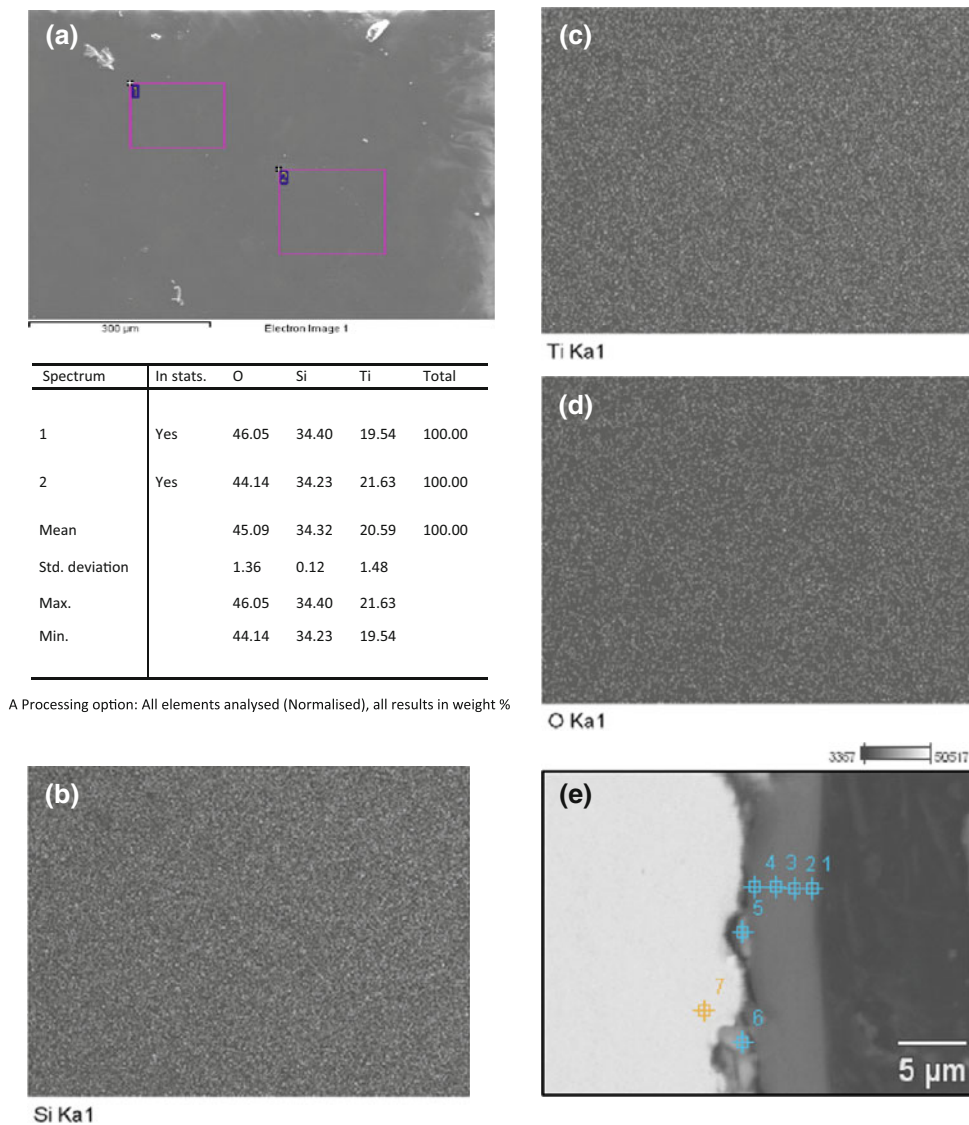


Fig. 5: (a) SEM–EDX photograph of Ti-coated sample, (b) distribution of Si particle, (c) distribution of Ti particle, (d) distribution of oxygen, and (e) cross-sectional view of coated sample

red rust spots). The EDX analysis of the red rust area as shown in Fig. 7 of the coated sample indicates the presence of Si, O, Fe, Na, and Cl ions, which indicates that chloride ion diffuses through coating matrix and an electrochemical reaction between iron and chloride and other available ions is initiated on the metal–solution interface. The absence of Ti particles in the red rust and blister areas indicates the existence of a strong Ti–O–Metal bond.

EIS study

The typical impedance spectra of the samples coated with titania-containing hybrid films after different intervals of time are presented in Fig. 8.

The numerical fittings with the appropriate equivalent circuits have been used in order to estimate the evaluation of corrosion protection properties for different sol–gel coated panels under study. The Randal equivalent circuits have been selected for fitting the experimental results based on the physico-chemical model of the corrosion process. The hybrid coatings demonstrate the highest resistance (1.7×10^4) R_{coat} at the beginning of immersion. However, this resistance decreases rapidly during the first 24 h of contact with 3.5% NaCl electrolyte solution. One well-defined time constant can be observed on the bode plots after 1 day immersion. The high frequency time constant is the result from the capacitance of the sol–gel layer. After several days of immersion one additional time constant appears on the impedance

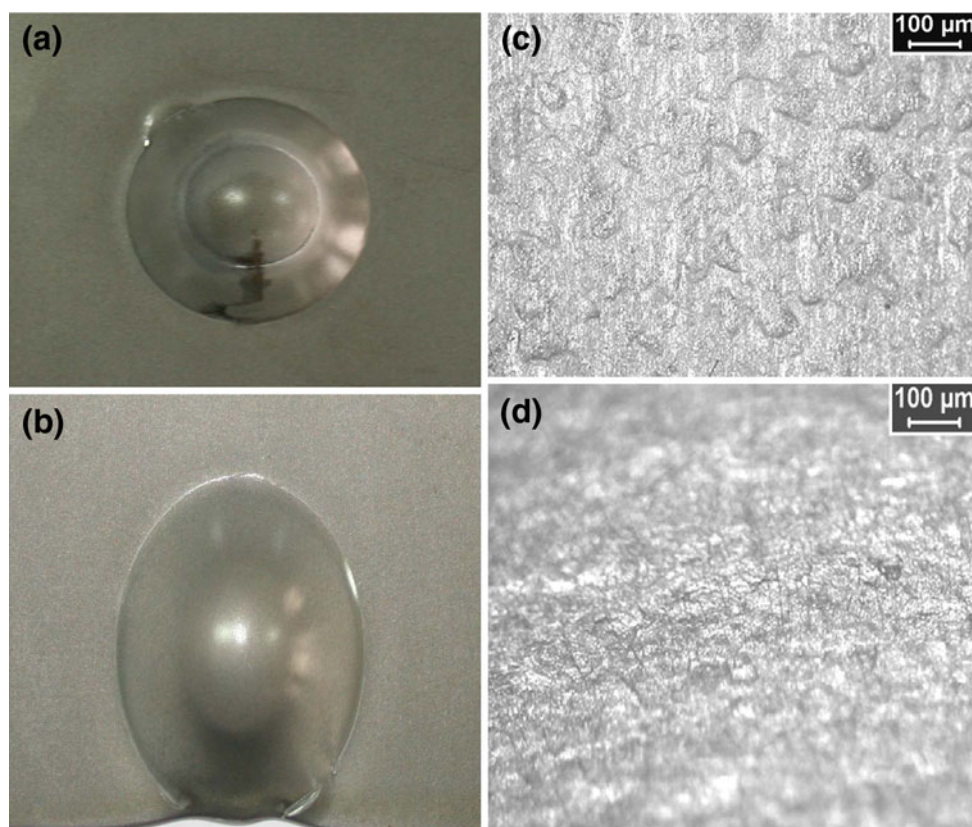


Fig. 6: Cupping test results: (a) coated sample after 9 mm cupping value, (b) coated sample after 7 mm cupping value, (c) SEM images of coated sample at 9 mm cupping value, and (d) SEM images of coated sample after 7 mm cupping value

spectrum in the low frequency region due to the onset of corrosion attack. Penetration of water molecules and chloride ions through the finest pores of the film is most probably responsible for this resistance drop.

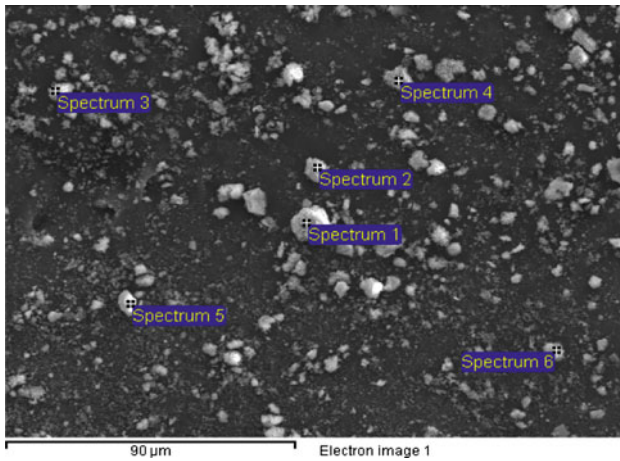
In addition to Bode plot analysis, barrier properties of the coating are also interpreted by impedance spectra using equivalent circuit, i.e., Randal model. The electrolyte solution resistance, R_s , is very low and it is ignored for further analysis. R_p is the coating resistance of the sol–gel coating, and C_f is the capacitance of the sol–gel coating. The variation of resistances and capacitances with the immersion time are shown in Table 1. The values of “Goodness-of-Fit” obtained with Gamry EIS 300 indicate an average error lying below 10%. The impedance value decreases gradually from $2.45E+5$ to $1.8E+4 \Omega/\text{cm}^2$ over 360 h of exposure in 3.5% NaCl solution. This shows much better corrosion resistance than glycidoxypropyl trimethoxy-based nanoTi sol–gel coatings.⁸ The good barrier properties of the coating are further confirmed from the almost constant coating capacitance (C_c) value. After 360 h exposure in 3.5% NaCl solution, C_c remains in the range of $E-9 \text{ F}/\text{cm}^2$. This reconfirms the existence of the strong three-dimensional polymeric network formed by the Ti–O–Metal, Si–O–Metal, and Ti–O–Si bond.^{21,31–34}

Polarization study

In order to compare the corrosion rate of nanohybrid titania sol–gel coating with bare steel surface, polarization curves for initial titania-coated sample, titania-coated sample after 360 h of exposure in 3.5% NaCl solution and bare CRCA sheet were measured and the corresponding results are shown in Fig. 9. From the above data one can find a substantial reduction in the value of corrosion current of sol–gel-coated specimen. Initial corrosion current for titania-coated sample is very much less than that of bare CRCA substrate; even after 360 h exposure in 3.5% NaCl solution titania-coated sample shows less corrosion current than bare substrate. High-contact angle, low-free surface energy and high T_g value contribute to the enhancement of the corrosion resistance.

Conclusion

Inorganic–organic hybrid sol for the corrosion protection coatings on CRCA has been prepared by sol–gel method by using titania-isopropoxide and *N*-phenyl-3-aminopropyl triethoxy silane. It has been observed that the hybrid coatings offer hydrophobic surface with



Processing option: All elements analysed (Normalised)

Spectrum	In stats.	O	Si	Cl	Fe	Total
Spectrum 1	Yes	38.18		0.65	61.17	100.00
Spectrum 2	Yes	36.35	1.34	1.56	60.75	100.00
Spectrum 3	Yes	44.82		0.82	54.37	100.00
Spectrum 4	Yes	46.51			53.49	100.00
Spectrum 5	Yes	41.25		2.32	56.43	100.00
Spectrum 6	Yes	45.14		0.84	54.02	100.00
Max.		46.51	1.34	2.32	61.17	
Min.		36.35	1.34	0.65	53.49	

All results in weight%

Fig. 7: SEM–EDX of Ti-hybrid-coated sample after 200 h salt spray test

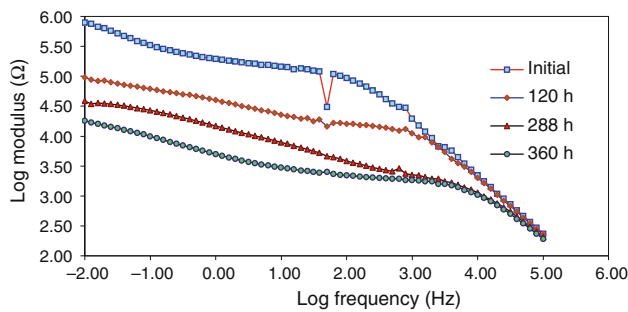


Fig. 8: EIS study of coated panel—Bode plot

good corrosion protection ability. High coating resistance of titania-coated substrate in 3.5% NaCl solution indicates that the coating is impervious to diffusion of water/corrosive ions. The improvement in protection is

Table 1: Coating resistance and capacitance at various immersion time (h)

Parameter study	2.2	3.2	4.5	6.1	24	216	288	339	360
Coating resistance, Ω/cm^2	2.455E+5	2.56E+5	4.98 E+5	3.0 E+5	5.97 E+4	1.81 E+4	34.548 E+4	1.814 E+4	1.829 E+4
Coating capacitance, F/cm^2	8.195E-9	8.124E-9	1.065E-8	8.436E-8	8.722E-9	8.911E-9	9.637E-9	9.870E-9	8.124E-9

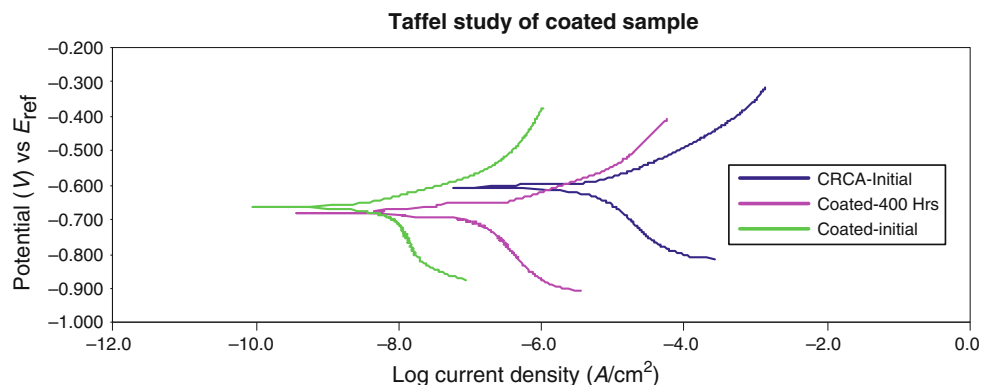


Fig. 9: Tafel polarization study of coated sample

due to the three-dimensional network of polycondensation of $\text{Ti}(\text{OH})_2$ and coupling agent. The improved adherence to the substrate is through H-bonds and van der Waals bonds between functionalized titania particles and metal substrate immediately after application. In addition to high corrosion resistance properties, further research can be focused on photocatalytic, antimicrobial and self-cleaning properties of titania sol-gel coatings.

Acknowledgments Authors would like to thank the Director RD &T, Tata Steel Limited for permission and encouragement to carry out this work and also acknowledge the valuable support of Mr. A. K. Singh provided during this work.

References

- Zheludkevich, ML, Salvado, IM, Ferreira, MGS, "Sol-Gel Coatings for Corrosion Protection of Metals." *J. Mater. Chem.*, **15** 5099–5111 (2005)
- Wang, D, Bierwagen, GP, "Sol-Gel Coatings on Metals for Corrosion Protection." *Prog. Org. Coat.*, **64** 327–338 (2009)
- Metroke, T, Wang, Y, Ooij, WJ, Schaefer, DW, "Chemistry of Mixtures of Bis-[Trimethoxysilylpropyl] Amine and Vinyltriacetoxysilane: An NMR Analysis." *J. Sol-Gel Sci. Technol.*, **51** 23–31 (2009)
- Twite, RL, Bierwagen, GP, "Review of Alternatives to Chromate for Corrosion Protection of Aluminum Aerospace Alloys." *Prog. Org. Coat.*, **33** 91–100 (1998)
- Metroke, TL, Parkhill, RL, Knobbe, ET, "Passivation of Metal Alloys Using Sol-Gel-Derived Materials—A Review." *Prog. Org. Coat.*, **41** 233–238 (2001)
- Khobaib, M, Reynolds, LB, Donley, MS, "A Comparative Evaluation of Corrosion Protection of Sol-Gel Based Coatings Systems." *Surf. Coat. Technol.*, **140** 16–23 (2001)
- Donley, MS, Mantz, RA, Khramov, AN, Balbyshev, VN, Kasten, LS, Gaspar, DJ, "The Self-Assembled Nanophase Particle (SNAP) Process: A Nanoscience Approach to Coatings." *Prog. Org. Coat.*, **47** 401–415 (2003)
- Sanchez, C, de Soler-Illia, GJAA, Ribot, F, Lalot, T, Mayer, CR, Cabuil, V, "Designed Hybrid Organic-Inorganic Nanocomposites From Functional Nanobuilding Blocks." *Chem. Mater.*, **13** 3061–3083 (2001)
- Hofacker, S, Mechtel, M, Mager, M, Kraus, H, "Sol-Gel: A New Tool for Coatings Chemistry." *Prog. Org. Coat.*, **45** 159–164 (2002)
- Zheludkevich, ML, Serra, R, Montemor, MF, Yasakau, KA, Salvado, IMM, Ferreira, MGS, "Nanostructured Sol-Gel Coatings Doped With Cerium Nitrate as Pre-treatments for AA2024-T3 Corrosion Protection Performance." *Electrochim. Acta*, **51** 208–217 (2005)
- Sanchez, C, Julian, B, Belleville, P, Popall, M, "Applications of Hybrid Organic-Inorganic Nanocomposites." *J. Mater. Chem.*, **15** 3559–3592 (2005)
- Judeinstein, P, Sanchez, C, "Hybrid Organic-Inorganic Materials: A Land of Multidisciplinary." *J. Mater. Chem.*, **6** (4) 511–525 (1996)
- Wei, Y, Bakthavatchalam, R, Whitecar, CK, "Synthesis of New Organic-Inorganic Hybrid Glasses." *Chem. Mater.*, **2** 337–339 (1990)
- Wouters, MEL, Wolfs, DP, van der Linde, MC, Hovens, JHP, Tinnemans, AHA, "Transparent UV Curable Antistatic Hybrid Coatings on Polycarbonate Prepared by the Sol-Gel Method." *Prog. Org. Coat.*, **51** 312–320 (2004)
- Bayramoglu, G, Kahraman, MV, Kayaman-Apohan, N, Gungor, A, "Synthesis and Characterization of UV-Curable Dual Hybrid Oligomers Based on Epoxy Acrylate Containing Pendant Alkoxysilane Groups." *Prog. Org. Coat.*, **57** 50–55 (2006)
- Zheludkevich, ML, Serra, R, Montemor, MF, Ferreira, MGS, "Oxide Nanoparticle Reservoirs for Storage and Prolonged Release of the Corrosion Inhibitors." *Electrochem. Commun.*, **7** 836–840 (2005)
- Zheludkevich, ML, Serra, R, Montemor, MF, Salvado, IMM, Ferreira, MGS, "Corrosion Protective Properties of Nanostructured Sol-Gel Hybrid Coatings to AA2024-T3." *Surf. Coat. Technol.*, **200** 3084–3094 (2006)
- Dhoke, SK, Khanna, AS, "Effect of Nano- Fe_2O_3 Particles on the Corrosion Behavior of Alkyd Based Waterborne Coatings." *Corros. Sci.*, **51** 6–20 (2009)
- Chou, TP, Chandrasekaran, C, Cao, GZ, "Sol-Gel-Derived Hybrid Coatings for Corrosion Protection." *J. Sol-Gel. Sci. Technol.*, **26** 321–327 (2003)
- Technical Data Sheet Granodine of M/S Henkel Chembond India Ltd.
- Lu, T, Blackburn, S, Dickinson, C, Rosseinsky, MJ, Hutchings, G, Axon, S, Leeke, GA, "Production of Titania

- Nanoparticles by a Green Process Route.” *Powder Technol.*, **188** 264–271 (2009)
22. Dholam, R, Patel, N, Adami, M, Miotello, A, “Physically and Chemically Synthesized TiO₂ Composite Thin Films for Hydrogen Production by Photocatalytic Water Splitting.” *Int. J. Hydrog. Energy*, **33** 6896–6903 (2008)
 23. Chau, JLH, Tung, C-T, Lin, Y-M, Li, A-K, “Preparation and Optical Properties of Titania/Epoxy Nanocomposite Coatings.” *Mater. Lett.*, **62** 3416–3418 (2008)
 24. Rout, TK, Bandyopadhyay, N, Narayan, R, Rani, N, Sengupta, DK, “Performance of Titania–Silica Composite Coating on Interstitial-Free Steel Sheet.” *Scr. Mater.*, **58** 473–476 (2008)
 25. Jordan, CE, Goggins, KM, Benscoter, AO, Marder, AR, “Metallographic Preparation Technique for Hot-Dip Galvanized and Galvannealed Coatings on Steel.” *Mater. Charact.*, **31** 107–114 (1993)
 26. Schraml-Marth, M, Walther, KL, Wokaun, A, “Porous Silica Gels and TiO₂/SiO₂ Mixed Oxides Prepared Via Sol-Gel Process: Characterization by Spectroscopic Techniques.” *J. Non-Cryst. Solids*, **143** 93–111 (1992)
 27. Aizawa, M, Nosaka, Y, Fujii, N, “Preparation of TiO₂-SiO₂ Glass Via Sol-Gel Process Containing a Large Amount of Chlorine.” *J. Non-Cryst. Solids*, **168** 49–55 (1994)
 28. Mukherjee, SP, “Sol–Gel Processes in Glass Science and Technology.” *J. Non-Cryst. Solids*, **42** 477–488 (1980)
 29. Rout, TK, “Electrochemical Impedance Spectroscopy Study on Multi-Layered Coated Steel Sheets.” *Corros. Sci.*, **49** 794–817 (2007)
 30. Karatas, S, Kızılkaya, C, Kayaman-Apohan, N, Gungor, A, “Preparation and Characterization of Sol–Gel Derived UV-Curable Organo-Silica–Titania Hybrid Coatings.” *Prog. Org. Coat.*, **60** 140–147 (2007)
 31. Seok, SI, Kim, JH, Choi, KH, Hwang, YY, “Preparation of Corrosion Protective Coatings on Galvanized Iron From Aqueous Inorganic–Organic Hybrid Sols by Sol–Gel Method.” *Surf. Coat. Technol.*, **200** 3468–3472 (2006)
 32. Zhu, Y, Ding, C, “Characterization of Plasma Sprayed Nano-Titania Coatings by Impedance Spectroscopy.” *J. Eur. Ceram. Soc.*, **20** 127–132 (2000)
 33. Rout, TK, “Nanolayered Oxide on a Steel Surface Reduces Surface Reactivity: Evaluation by glow Discharge Optical Emission Spectroscopy (GDOES).” *Scr. Mater.*, **56** 573–576 (2007)
 34. Valente, T, Galliano, FP, “Corrosion Resistance Properties of Reactive Plasma-Sprayed Titanium Composite Coatings.” *Surf. Coat. Technol.*, **127** 86–92 (2000)